Influence of 5′-Nearest Neighbors on the Insertion Kinetics of the Fluorescent Nucleotide Analog 2-Aminopurine by Klenow Fragment†

Linda B. Bloom,‡ Michael R. Otto,§ Joseph M. Beechem,§ and Myron F. Goodman*,‡

Department of Biological Sciences, Molecular Biology Section, University of Southern California, Los Angeles, California 90089-1340, and Department of Molecular Physiology and Biophysics, Vanderbilt University, Nashville, Tennessee 37232-0615

Received April 29, 1993; Revised Manuscript Received August 11, 1993®

ABSTRACT: The effects of nearest neighbor interactions between a nucleotide base at the primer 3′-terminus and an incoming deoxyribonucleoside triphosphate on DNA polymerase catalyzed insertion were examined. Kinetics of inserting the fluorescent nucleotide analog 2-aminopurine deoxyribonucleotide (dAPMP) and dAMP opposite a template T by 3′→5′ exonuclease-deficient mutants of Klenow fragment (KF⁻) were measured on primer/templates of identical sequence except for the base pair at the 3′-primer terminus. In addition to its fluorescence properties, 2-aminopurine (AP) is an attractive probe because it is misinserted opposite T by polymerases at much higher frequencies than natural nucleotides. Misinsertion frequencies for AP are on the same order of magnitude as variations in misinsertion frequencies due to changes in local DNA sequence, which makes the statistical significance of these variations easier to document. We have established that changes in the fluorescence of AP can be used to follow the insertion of dAPMP on both steady-state and pre-steady-state time scales. Rates of insertion of dAPMP measured by fluorescence and by a polyacrylamide gel assay were similar and are sensitive to the identity of the base at the 3′-primer terminus. The rate of inserting dAPMP following a primer terminus G, C, or A was twice as fast as insertion following a primer terminus T. The difference in rates arises primarily from differences in k_{cat} values, which were fastest next to G and slowest next to T, while apparent K_m values were similar next to each of the 4 different nearest neighbors. The gel assay was used to measure AP misinsertion efficiencies by two methods: (1) by having dAPTP and dATP directly compete for insertion opposite T in the same reaction and (2) by measuring V_{max}/K_m values for each substrate in separate reactions. The results from the direct competition and separate kinetics measurements are similar. The misinsertion efficiency of dAPMP relative to dAMP opposite a template T was significantly higher next to a 3′-primer terminus G ($f_{ins} = 0.31 \pm 0.06$) than next to T ($f_{ins} = 0.15 \pm 0.03$) for the KF⁻ single mutant (D424A). The corresponding misinsertion efficiencies next to a 3′-primer terminus G and T were 0.20 ± 0.02 and 0.16, respectively, for the KF⁻ double mutant (D355A, E357A). Relative rates of insertion of dAPMP and dAMP correlate with melting temperatures calculated for nearest neighbor doublets which reflect the relative base-stacking energies. In addition to changes in insertion kinetics, polymerase–DNA dissociation rates varied with the identity of the 3′-primer terminus, differing by as much as 7–20-fold depending on the polymerase and the primer/template.

DNA polymerases copy DNA with "average" nucleotide insertion error rates in a 10^{-3}–10^{-5} range for all possible transition and transversion mispairs; for a review, see Echols and Goodman (1991). There is, however, significant site-to-site variability in misinsertion rates, by an order of magnitude or more, depending on surrounding nucleotide sequence (Mendelman *et al.*, 1989). Since a DNA primer/template occupies the binding site where the nucleotide to be incorporated binds, it is not surprising that the local DNA sequence can affect nucleotide insertion fidelity. Nucleotide sequences at sites immediately before and after the site where insertion occurs are likely to have the largest effect on the interactions between an incoming dNTP and the enzyme–DNA complex. Base-stacking interactions between the incoming nucleotide and the nucleotide at the primer terminus (5′-nearest neighbor) may affect enzyme–DNA–dNTP complex stability, resulting in variation in the relative efficiencies of forming correct and incorrect base pairs.

Although it is clear that local DNA sequence can contribute to the frequency of misincorporation (Joyce *et al.*, 1992; Mendelman *et al.*, 1989; Pless & Bessman, 1983), a systematic study to elucidate the effects of specific sequence changes on nucleotide insertion and excision has not been presented. In this paper, the influence of the 5′-nearest neighbors on the efficiency of nucleotide insertion by 3′→5′ exonuclease deficient mutants of Klenow fragment (KF⁻) was examined. Recent studies with KF⁻ have shown that both nucleotide insertion and extension are influenced by the local DNA sequence context (Joyce *et al.*, 1992), although correlations between DNA sequence and fidelity still remain to be identified.

The nucleotide analog 2-aminopurine 2′-deoxyribonucleoside 5′-triphosphate (dAPTP,[1] Chart I) was used as a probe to evaluate the effects of local DNA sequence on misinsertion. Although 2-aminopurine is capable of forming a Watson–

† This work was supported by NIH Grant GM21422 (M.F.G.), by NIH Postdoctoral Fellowship GM15034 (L.B.B.), and by NIH Training Grant T32GM08320 (M.R.O.). J.M.B. is a Lucille Markey Scholar in Biomedical Sciences.

‡ University of Southern California.

§ Vanderbilt University.

® Abstract published in *Advance ACS Abstracts,* October 1, 1993.

0006-2960/93/0432-11247$04.00/0

Chart I: Structures of A·T and AP·T Base Pairs

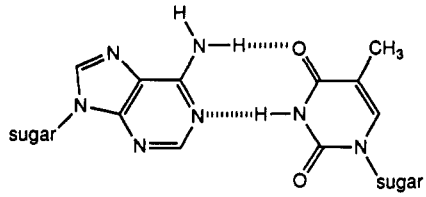

A·T

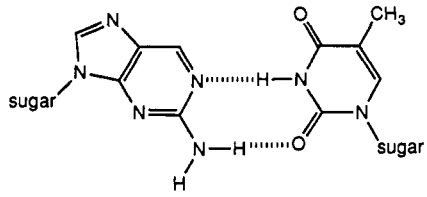

AP·T

Crick type base pair with thymine (Sowers *et al.*, 1986), polymerases are still able to discriminate between insertion of 2-aminopurine and adenine opposite thymine, but misinsertion frequencies for AP are much higher than for natural nucleotides on the order of 10–15% (Bessman *et al.*, 1974; Clayton *et al.*, 1979; Pless & Bessman, 1983). For natural nucleotides, differences in the relative rates of correct and incorrect insertion are very large, on the order of a factor of 10^3–10^5, in comparison with differences in rates within different sequence contexts, which may vary by as much as a factor of 10 or more (Mendelman *et al.*, 1989). Evaluating differences between correct and incorrect insertion for natural nucleotides within different sequence contexts would require measuring relatively small differences in the ratio of a very large number to a very small number. Variations in the misinsertion frequency of AP due to changes in the local DNA sequence are likely to be on the same order of magnitude as the misinsertion frequency, making AP a more sensitive probe for measuring the effects of local DNA sequence on insertion. The kinetics of insertion of dAPMP and dAMP opposite T and their relative insertion efficiencies were measured on synthetic primer/templates (Chart II) having identical sequence except for the base pair immediately 5′ to the incoming dNTP, so that the effects of nearest neighbor interactions could be evaluated in the absence of the other sequence context effects.

A second advantage of using AP as a probe is that it is much more fluorescent than natural nucleotides, and its fluorescence properties are sensitive to its environment. We have shown that changes in the fluorescence intensity of AP can be used to follow polymerase-catalyzed insertion. A comparison is made between two methods for measuring the kinetics of DNA polymerase catalyzed reactions. In the first method, changes in the fluorescence intensity of AP as it was incorporated into DNA were used to measure reaction kinetics on pre-steady-state and steady-state time scales. The second method uses a gel assay system (Boosalis *et al.*, 1987; Goodman *et al.*, 1993) to measure incorporation of both AP and A deoxyribonucleotides.

[1] Abbreviations: dAPTP, 2-aminopurine 2′-deoxyribonucleoside 5′-triphosphate; AP, 2-aminopurine; dNTP, 2′-deoxyribonucleoside 5′-triphosphate; KF⁻, a 3′→5′ exonuclease-deficient mutant of the large (Klenow) of *Escherichia coli* DNA polymerase I; KF⁺, Klenow fragment with the 3′→5′ exonuclease activity present; DTT, dithiothreitol; BSA, acetylated bovine serum albumin; DMT, dimethoxytrityl protecting group; CPG, controlled-pore glass.

Chart II: Sequences of Primer/Templates

primer templates for standing start reactions:

```
16mer:  5'- TCC CAG TCA CGA CGT Y
30mer:  3'- AGG GTC AGT GCT GCA XTZ GTA CGA GCT ACT
```

primer templates for running start reactions (universal primer, up):

```
15mer:  5'- TCC CAG TCA CGA CGT
30mer:  3'- AGG GTC AGT GCT GCA XTZ GTA CGA GCT ACT
```

primer (p)	Y	template (t)	X	Z
pG	G	tC	C	A
pC	C	tG	G	A
pA	A	tT	T	A
pT	T	tA_1	A	A
up		tA_2	A	G

EXPERIMENTAL PROCEDURES

Materials

KF⁻ (D424A) was a kind gift from Dr. Catherine M. Joyce (Derbyshire *et al.*, 1991). Klenow exo⁻ (D355A, E357A) was either purified (Derbyshire *et al.*, 1988; Joyce & Grindley, 1983) from an overproducing strain provided by Dr. Catherine M. Joyce or purchased from U.S. Biochemical Corp. KF⁻ solutions were diluted for storage in a buffer consisting of 20 mM Tris, pH 7.5, 0.5 mM dithiothreitol, 1 mg/mL BSA, and 50% glycerol. Concentrations of KF⁻ were determined by measuring the absorbance at 278 nm ($\epsilon = 6.32 \times 10^4$ M^{-1} cm^{-1} (Setlow *et al.*, 1972)), and concentrations of KF⁻ from US Biochemical Corp. were determined from specific activities and protein concentrations. Acetylated bovine serum albumin was purchased from U.S. Biochemical Corp. Restriction enzymes *Mbo*I, *Dde*I, and *Hin*fI were purchased from Pharmacia, and *Exo*III was purchased from Boehringer Mannheim. FPLC-purified dNTPs were purchased from Pharmacia LKB Biotechnology, Inc., and used without further purification. Oligonucleotides were synthesized on an Applied Biosystems Model 381A DNA synthesizer using standard 2-cyanoethyl phosphoramidite chemistry and purified by denaturing polyacrylamide gel electrophoresis. Nucleotide sequences are given in Chart II and referred to by their designations throughout the text. A DMT-protected 2-aminopurine was linked to a solid support (CPG) for preparation of oligos containing AP at the 3′-terminus (Eritja *et al.*, 1986). dAPTP was prepared as described previously (Bessman *et al.*, 1974; Clayton *et al.*, 1979). Concentrations of dAPTP were determined by measuring the absorbance at 304 nm ($\epsilon = 5800$ M^{-1} cm^{-1}).

Methods

Time-Resolved Measurements. Time-resolved experiments were performed with free dAPTP and with a synthetic primer/template of identical sequence to pT/tA_1 but containing AP at the 3′-primer terminus. Free dAPTP data was collected at 0.5 μM in 50 mM Tris-HCl, pH 7.4, and the AP primer/template data was collected in 25 mM HEPES and 50 mM NaCl. KF⁻–DNA complex measurements were made on a solution containing 1 μM KF⁻ (D355A, E357A), 0.5 μM pG/tC, 0.5 mM EDTA, 25 mM HEPES, pH 7.5, and 50 mM NaCl.

Time-resolved fluorescence measurements were performed utilizing a Coherent Antares Nd:YAG laser (Palo Alto, CA), frequency doubled and synchronously pumping a dual dye-jet laser (Coherent 702) using rhodamine 6G and a DODCI saturable absorber. Output pulses from this laser at 306 nm were utilized at 4 MHz and had a pulse width of approximately 1 ps. Time-resolved detection utilized time-correlated single-

photon counting with a 6-μm Hamamatsu (R2809U-01, Bridgewater, NJ) microchannel plate detector, high-frequency 50X amplifiers (Phillips Scientific 774, Mahwah, NJ), constant fraction discriminators (Tennelec 454, Oak Ridge, TN), time-to-amplitude converters (Tennelec 862), and pulse-height analysis analog-to-digital converters (Nucleus PCA-II, Oak Ridge, TN). The instrument response function was approximately 50–100 ps. The collimated fluorescence emission was passed through Glan-Thompson polarizers on automated mounts (ISS, Urbana, IL) and focused onto the entrance slits of a SPEX (Edison, NJ) 0.22-m emission monochromator. A half-wave plate in the excitation beam was utilized to rotate the excitation polarization to horizontal for the determination of the polarization bias ("*g*-factor") of the detection instrumentation.

Quantum Yield Determination. A SPEX Fluorolog 1681 fluorimeter was used to measure quantum yields. Emission spectra were collected for solutions of 4 μM primer/template or dAPTP in 25 mM HEPES and 50 mM NaCl, pH 7.5 between 330 and 460 nm at 0.5-nm intervals and integrated over 0.5 s. Buffer background signals were subtracted from spectra. Relative quantum yield values were calculated by dividing the integral of the primer/template fluorescence by that of the dAPTP fluorescence. Absolute quantum yield values were obtained by multiplying relative values by the reported quantum yield of 0.63 for dAPTP (Ward *et al.*, 1969).

Fluorescence Detection. Fluorescence detection from the stopped-flow apparatus consisted of a home-built single-photon detector consisting of the following: Hamamatsu R928 photomultiplier, 5X 300-MHz amplifier (Stanford Research SR445, Sunnyvale, CA), discriminator (Stanford Research SR400), and multichannel scaler (Tennelec Model MCS-II, Oak Ridge, TN), interfaced to an 80486 microcomputer. The detection system was activated from an external synch-out pulse from the Molecular Kinetic stepper-motor controlling unit, and data acquisition began at least 100 ms before sample mixing. Data was collected at time bases from 1 ms to 1 s in 8000 total channels. Fluorescence excitation utilized a 75-W xenon arc lamp (Oriel, Stratford, CT) coupled to a 0.25-m monochromator (Oriel 77250) with fiber optic output directed into the 75-μL-volume sample cell. Excitation wavelength was 311 nm, and emission was collected through a 360-nm cut-on filter (Hoya Optics type L36, Fremont, CA).

Fluorescence Determination of Steady-State Kinetic Constants Using Standing-Start Primer/Templates. Reactions were perfomed using rapid mixing techniques in a Molecular Kinetic (Pullman, WA) three-syringe stepper-motor-controlled stopped-flow apparatus. Rate of product formation was determined from the decrease in the steady-state dAPTP fluorescence. Apparent K_m and V_{max} values were obtained using the method described below under Calculation of Kinetic Constants. Stock solutions of dAPTP, a dilution buffer, and primer/template–KF^- were placed in separate syringes. Reactions were perfomed at 19 ± 2 °C by mixing an aliquot of dAPTP with dilution buffer and then mixing 300 μL of the diluted dAPTP solution with 150 μL of primer/template–enzyme stock solution. Volumes of the dAPTP and dilution buffer solutions were varied between 0 and 300 μL to give desired dAPTP concentrations, which varied as per template and are listed below. All reactions contained final concentrations of 50 mM Tris-HCl, pH 7.4, 5 mM $MgCl_2$, 0.3 mM DTT, 0.03 mg/mL BSA, 5 nM KF^- (D355A, E357A), and 70 nM standing-start primer/template (Chart II). Template tA_2: Low- (0.75 μM) and high-concentration dAPTP (2.25 μM) stock solutions were used to ramp the concentration from 0.1 to 0.5 and from 0.6 to 1.5 μM, respectively. Template tC: A 1.5 μM dAPTP stock solution was used to vary the concentration from 0.2 to 1.0 μM. Templates tA_1, tT, and tG: A 0.75 μM dAPTP stock solution was used to ramp concentrations from 0.1 to 0.5 μM, and a 3.75 μM dAPTP stock solution was used for 0.75 to 2.5 μM dAPTP concentrations. For these last three templates multiple runs (2–3) were summed to increase signal to noise.

Saturated Steady-State Kinetics. A more fully saturated steady-state experiment was run using the pC/tG primer/template. Four dAPTP stocks were used in this experiment of 2.0, 8.0, 16, and 24 μM to vary dAPTP concentration from 0.5 to 12 μM. Reactions were otherwise identical with the steady-state experiments above except that the pC/tG concentration was 0.5 μM. At the higher dAPTP concentrations multiple (2–5) runs were summed to increase signal to noise.

Fluorescence Determination of Pre-Steady-State Kinetic Constants. Reactions were performed in the stopped-flow apparatus at 19 ± 2 °C. Primer/template–KF^- (D355A, E357A) solutions were prepared which contained 0.1 mg/mL BSA and 1 mM DTT. Reactions were initiated by mixing equal volumes (150 or 180 μL) of primer/template–KF^- solution with dAPTP/dilution buffer solution. All reactions contained 50 mM Tris-HCl, pH 7.4, and 8 mM $MgCl_2$. Final concentrations of dAPTP in reactions ranged from 0.6 to 1.8 μM for pC/tG and 0.6 to 3.6 μM for pT/tA_1. Final concentrations of primer/template and KF^- were 300 and 100 nM. Pre-steady-state kinetics were obtained at high dAPTP concentrations for primer/templates pC/tG and pT/tA_1 using 0.2 μM Klenow fragment, 0.5 μM DNA, and 10 μM dAPTP. Reactions were initiated as above by mixing 120 μl of 0.4 μM Klenow fragment and 1.0 μM DNA mixed with 120 μl of 20 μM dAPTP. Multiple experiments were summed (approximately 30 runs) to obtain acceptable signal to noise.

Single-Turnover Pre-Steady-State Experiment. Reaction conditions were as for pre-steady-state experiments unless stated otherwise. Final concentrations were 1.0 μM and 0.5 μM for KF^- (D355A, E357A) and pT/tA_1, respectively. Four dAPTP stocks of 2.0, 8.0, 16, and 24 μM were used to ramp dAPTP concentrations from 0.5 to 12 μM. All velocities above 4 μM dAPTP were summed results from multiple experiments.

Calculation of Kinetic Constants. All fluorescence reactions were normalized to total change in AP fluorescence because the amount of AP fluorescence quench seen varied between the four different primer/templates. Initial velocities were obtained directly by calculating the slope of the initial part of the reactions. For steady-state reactions, k_{cat} and K_m values were calculated from plots of observed initial rates versus dAPTP concentration. For pre-steady-state reactions, kinetic constants were calculated by assuming the pathway below, which is described by the rectangular hyperbola in eq 1:

$$KF^-\cdot DNA + dAPTP \overset{K_m}{\rightleftharpoons} KF^-\cdot DNA\cdot AP \xrightarrow{k_{cat}} KF^-\cdot DNA_{+1}\cdot PP_i$$

$$k_{obs} = \frac{k_{cat}[dAPTP]}{K_m + [dAPTP]} \approx \frac{k_{cat}}{K_m}[dAPTP] \qquad (1)$$

At high concentrations of dAPTP in comparison to DNA, the change in the large dAPTP signal was small and the resulting noise in data points was large. At lower concentrations of dAPTP where individual data points are more reproducible, plots of k_{obs} versus [dAPTP] showed a small amount of curvature. Because of the signal-to-noise problems, separate values of k_{cat} and K_m were not extracted. Instead plots of k_{obs}

versus [dAPTP] were fit to the linear approximation in eq 1. However, it is clear that rates and kinetic constants determined by using pre-steady-state kinetic measurements were similar to those obtained from steady-state measurements.

Preparation of DNA Trap. Calf thymus trap DNA was prepared as described (Joyce, 1989) except that the DNA was sheared before enzymatic digestion by passing it through a narrow-bore needle several times and that the restriction enzyme *Mbo*I was substituted for *Sau*3AI.

Single-Hit Kinetic Measurements in the Presence of Trap DNA. Primer 5′-end labeling using 0.5 equiv of [γ-^{32}P]ATP, annealing, electrophoresis, and data analysis were done as described by Boosalis *et al.* (1987) except that a Molecular Dynamics PhosphorImager was used to determine the intensities of gel bands rather than autoradiography and densitometry. Nucleotide solutions for kinetics were prepared by mixing a 10× Klenow reaction buffer consisting of 0.50 M Tris, pH 7.4 at 20 °C, 60 mM $MgCl_2$, and 5 mM dithiothreitol with 10× solutions of dNTPs and dH_2O to give 1× concentrations when finally diluted in kinetics reactions. KF$^-$ (D424A) was diluted 1:10 in a solution of 0.2 mg/mL BSA and 1 mM dithiothreitol. Kinetics reactions were initiated by mixing 4 μL of a dNTP/trap DNA solution consisting of equal volumes of dNTP solution and a solution of 4 mg/mL trap DNA with 4 μL of primer/template–Klenow solution consisting of equal volumes of labeled DNA and diluted KF$^-$ solution. After 15 s at 20 °C, reactions were quenched with 24 μL of 20 mM EDTA in 95% formamide. Final concentrations of KF$^-$ (D424A), primer/template, and trap DNA were 23 nM, 50 nM, and 1 mg/mL, respectively. Final concentrations of running-start bases were 40 μM for dTTP, 20 μM for dCTP, and 5.5 μM for dGTP. Concentrations of dATP were varied between 0.085 and 19 μM, and concentrations of dAPTP were varied between 0.11 and 57 μM.

Control reactions were performed with up (universal primer)/tA_2 by incubating the reactions for 5, 15, 30, and 45 s to ensure that a 15-s reaction time was long enough for the polymerase reaction to be completed. Control reactions were performed to determine the effectiveness of the DNA trap by preincubating the DNA primer/template and trap DNA before adding polymerase and dNTP solutions. The percentages of primer extension observed when the primer/templates were preincubated with trap DNA were not greater than 2% of the percentages of primer extension observed in kinetics reactions.

Reactions with the KF$^-$ double mutant (D355A, E357A) contained 12 nM KF$^-$, 50 nM primer/template, and 1 mg/mL trap DNA. Polymerase was diluted 1:10 in a solution that contained final concentrations of 0.18 mg/mL BSA, 0.7 mM DTT, and 2× Klenow reaction buffer. Nucleotide/trap DNA solutions and KF$^-$/DNA solutions were made as above, and reactions were performed as described above. Final concentrations of the running-start bases were 6.7 μM for dTTP, 6.9 μM for dCTP, and 6.8 μM for dGTP. Concentrations of dATP ranged from 0.085 to 18.7 μM, and concentrations of dAPTP ranged from 0.22 to 57 μM.

Measurement of Polymerase–DNA Dissociation Rates. Nucleotide and primer/template–polymerase solutions were prepared as described for the kinetics measurements in the presence of trap DNA. Reactions were initiated by mixing 4 μL of the running-start dNTP/trap DNA solution with 4 μL of the primer/template–Klenow solutions at 20 °C. After delay times between 3 and 150 s, a solution of a saturating concentration of dATP in 1× Klenow reaction buffer was added to the reaction mixture, and the reaction was quenched after 15 s with 30 μL of 20 mM EDTA in 95% formamide. For a 0-s delay time reaction, a dNTP/trap DNA solution was prepared which contained both the running-start dNTP and dATP, and 4 μL of this solution was added to 4 μL of primer/template–enzyme solution before the reaction was quenched at 15 s. Final concentrations of KF$^-$ (D424A), primer/template, and trap DNA were 23 nM, 50 nM, and 1 mg/mL, respectively. Measurements were made twice for each primer/template. Nucleotide concentrations were as follows for the different primer/templates: 40 μM dTTP and 50 or 51 μM dATP for up/tA_1 and up/tA_2, 20 μM dCTP and 26 or 51 μM dATP for up/tG, and 5.6 μM dGTP and 26 or 51 μM dATP for up/tC. For reactions with the KF$^-$ double mutant (D355A, E357A), final concentrations of KF$^-$, primer/template, and trap DNA were 12 nM, 50 nM, and 1 mg/mL, respectively. Each reaction mixture contained 51 μM dATP and the following concentrations of running-start nucleotide: 6.7 μM dTTP for up/tA_1, 6.9 μM dCTP for up/tG, and 6.8 μM dGTP for up/tC.

Values for the dissociation rate constants, k_{off}, were determined by fitting the fraction of primers extended from the site before the target site (site $i-1$) to the target site (site i) as a function of time to a first-order exponential decay (see Figure 4). Control reactions in which primer/templates were preincubated with trap DNA before dNTPs and polymerase were added were performed with delay times between 10 and 120 s to ensure that the trap was effective throughout the entire time course of the reactions. The percentages of primers extended in the control reactions at the longest delay times used in the reactions were not greater than 2% of the percentages of primers extended in k_{off} reactions.

Measurements of k_{off} in the presence of GTP which is not incorporated were done as above, using 25 nM KF$^-$ (D355A, E357A), 50 nM up/tA_1, 1 mg/mL BSA, 49 μM dTTP, and 51 μM dATP. GTP was added to the dTTP/trap DNA solutions to give final concentrations of 0, 60, and 250 μM GTP. KF$^-$ was diluted 1:10 in a solution containing final concentrations of 0.18 mg/mL BSA and 0.9 mM DTT before it was added to primer/template.

Direct Competition. Primer 5′-end labeling, annealing, electrophoresis, and data analysis were done as described above for insertion kinetics. Nucleotide/trap DNA solutions and KF$^-$ (D355A, E357A)/primer/template solutions were prepared as for the separate kinetics measurements, and the general procedure was the same as that used for separate kinetics. Final concentrations of KF$^-$, up/tC, trap DNA, and dGTP were 12 nM, 50 nM, 1 mg/mL, and 6.8 μM, respectively. Each reaction mixture contained 0.17 μM dATP and concentrations of dAPTP ranging from 0.11 to 14.5 μM. Reactions were quenched after 15 s. Primers ending in either A or AP can be separated by running on a 16% polyacrylamide gel at room temperature; see Figure 5.

The misinsertion efficiency of AP, $f_{ins} = (k_{cat}/K_m)_{AP}/(k_{cat}/K_m)_A$, can be calculated from the fraction of primers extended by A in the presence of competing AP as derived below. The fraction of primers extended by dAMP in the presence of dAPMP is given by the relative rates of insertion of A and AP, as in eq 2,

$$\frac{I_A}{I_A + I_{AP}} = \frac{(k_{cat}/K_m)_A[A]}{(k_{cat}/K_m)_A[A] + (k_{cat}/K_m)_{AP}[AP]} \quad (2)$$

where $I_{A\ and}\ I_{AP}$ are the band intensities for primers ending in A and AP, respectively, and [A] and [AP] are the concentrations of dATP and dAPTP, respectively.

Misinsertion efficiencies were calculated by rearranging eq 2 to eq 3 and fitting the observed band intensities at each

dAPTP concentration to eq 3.

$$\frac{I_A}{I_A + I_{AP}} = \frac{[A]}{[A] + \frac{(k_{cat}/K_m)_{AP}}{(k_{cat}/K_m)_A}[AP]} \quad (3)$$

The misinsertion efficiency calculated from direct competition using eq 3 can be compared to the values of k_{cat}/K_m obtained by measuring the incorporation of dAMP as a function of [dATP] and of dAPMP as a function of [dAPTP] in separate experiments, i.e., in the absence of direct competition.

RESULTS

To investigate the effects of nearest neighbor interactions on nucleotide insertion kinetics and fidelity, we measured the misinsertion of dAPMP and the correct insertion of dAMP opposite a template T in synthetic oligonucleotide primer/templates of identical sequence except for the nucleotide at the 3′-primer terminus (5′-nearest neighbor). Kinetic studies of insertion were done by two methods. The first method monitored changes in the fluorescence of AP during polymerase-catalyzed incorporation of dAPMP at millisecond intervals. The second method used a gel assay to measure the kinetics for insertion of dAPMP or dAMP opposite T (Boosalis *et al.*, 1987; Goodman *et al.*, 1993), from which the AP misinsertion efficiency can be deduced (Fersht, 1985). Alternatively, the gel assay can be used to measure the AP misinsertion efficiency directly by allowing the two substrates to compete for insertion into DNA.

Insertion of dAPMP by KF⁻ was measured next to the four common 5′-nearest neighbor nucleotides. Oligonucleotide sequences are shown in Chart II. Insertion of dAPMP opposite T in an oligonucleotide primer/template that differs in the identity of the base 5′ to the template T site (template tA_2) was also examined to measure the effect of cross stacking on insertion. The majority of the fluorescence measurements were done using standing-start primer/templates (Chart II) where the oligonucleotide primer ends at the site immediately before the template target T site. In the gel assay, running-start primer/templates (Chart II) were used where insertion of one nucleotide is required to extend the primer to the target T site. Mutants of the large fragment of DNA polymerase I which were deficient in their 3′→5′ exonuclease activity, KF⁻, were used in this study so that the insertion kinetics were not complicated by exonucleolytic removal of inserted nucleotides. Two different exonuclease deficient mutants, one having a single amino acid substitution (D424A) and the other having two amino acid substitutions (E355A, D357A), were examined.

Fluorescence Properties of 2-Aminopurine. The fluorescence emission of AP is sensitive to its environment (Ward *et al.*, 1969). When AP is present as a deoxyribonucleoside triphosphate, its steady-state emission is about 25–125 times greater, depending on surrounding sequence, than when present at a primer 3′-terminus. When AP is present at the 3′-terminus of double-stranded DNA, its emission is quenched relative to single-stranded DNA (Figure 1a). The excitation maximum for AP is at 310 nm, and the emission maximum is at 365 nm, for both the free nucleotide and the nucleotide incorporated into DNA.

The fluorescence emission intensity is sensitive to the nearest neighbor base-stacking partner for AP. The intensities decrease as the base-stacking partner for AP is changed in the order T ≈ A > C > G. Quantum yields for AP within these primer/templates relative to free dAPTP are 3.7, 3.5, 2.4, and 0.8% for tA_1, tT, tG, and tC templates, respectively. Using the quantum yield of 63% reported for dAPTP (Ward *et al.*, 1969) gives absolute quantum yields for AP within these primer/templates of 2.3, 2.2, 1.5, and 0.5% for templates tA_1, tT, tG, and tC, respectively. Time-resolved fluorescence emission and anisotropy decays for AP are sensitive to the environment. The fluorescence intensity of free dAPTP in solution decays as a single exponential with a lifetime of 8.57 ns compared to 10.43 ns previously reported for the nucleoside

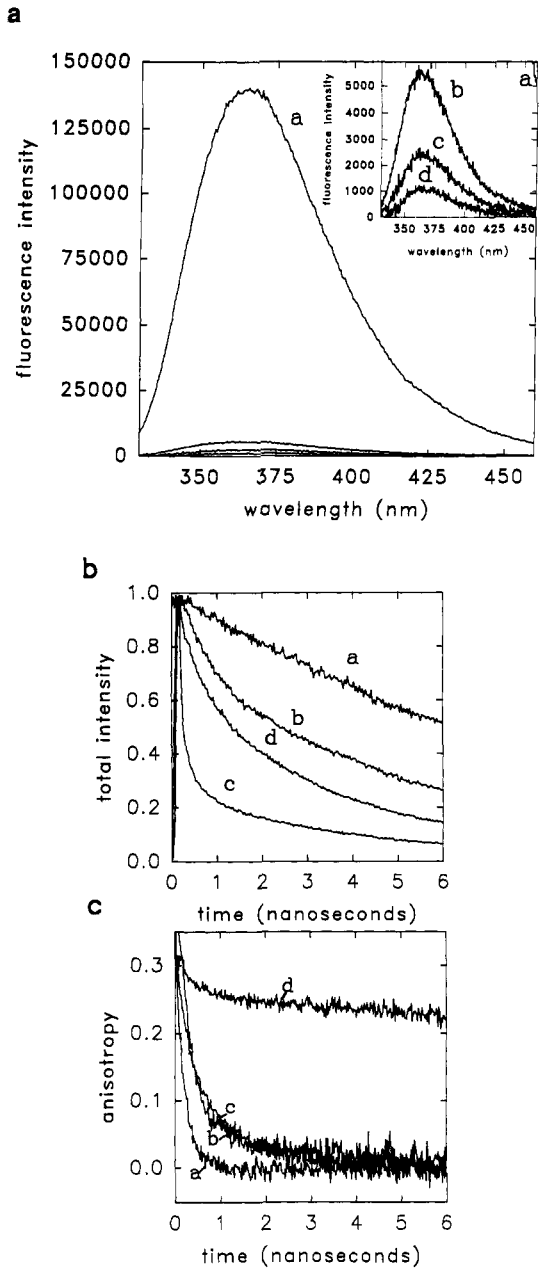

FIGURE 1: Steady-state fluorescence emission spectra and time-resolved total intensity and anisotropy decays for AP in different environments. Conditions are described in Methods. (Panel a) Steady-state fluorescence emission spectra for dAPTP (a), a synthetic single-stranded oligo of identical sequence to pG but containing AP at the 3′-terminus (b), KF⁻(D355A, E357A) bound to a duplex made up of the AP primer in spectrum b annealed to template tC (c), and the synthetic AP-containing duplex free in solution (d). The inset shows the less intense spectra on an expanded scale. (Panel b) Time-resolved total intensity decays for dAPTP (a), a synthetic 17mer oligo of identical sequence to pC with the addition of AP at the 3′-terminus (b), a duplex consisting of the primer in spectrum b annealed to template tG (c), and a duplex of the same sequence as pG/tC containing AP at the 3′-terminus bound to KF⁻ (d). (Panel c) Time-resolved anisotropy decays for the AP species in panel b.

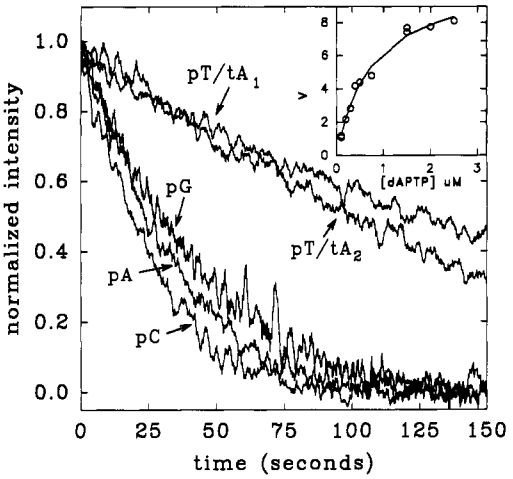

FIGURE 2: Time courses for steady-state incorporation of dAPMP into each of the five primer/templates. Reactions were performed at 20 °C using 5 nM KF⁻ (D355A, E357A), 70 nM primer/templates, and 0.2 μM dAPTP as described in Methods. The inset shows a plot of observed reaction rate versus concentration of dAPTP for reactions containing 5 nM KF⁻ (D355A, E357A) and 70 nM pC/tG as described in Methods.

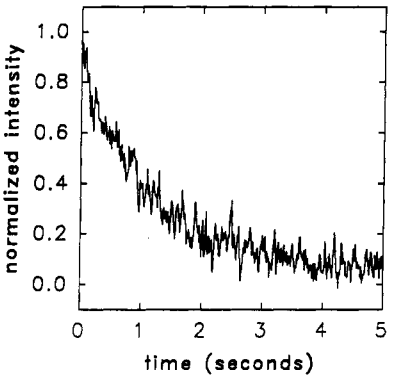

FIGURE 3: Pre-steady-state kinetics of insertion of dAPMP into pC/tG by KF⁻ (D355A, E357A) at 20 °C as described inMethods. Concentrations of KF⁻, DNA, and dAPTP were 200 nM, 500 nM, and 10 μM, respectively.

Table I: Steady-State Kinetic Constants for Insertion of dAPMP opposite a Template T Determined by Fluorescence Spectroscopy[a]

primer/ template	5′-nearest neighbor	K_m (μM)	k_{cat} (s^{-1})	k_{cat}/K_m (μM^{-1} s^{-1})	slope[b] (μM^{-1} s^{-1})
pG/tC	G	1.1 ± 0.40	2.0 ± 0.49	1.8	1.3
pC/tG	C	0.78 ± 0.09	1.5 ± 0.08	2.0	1.4
pA/tT	A	0.81 ± 0.11	1.3 ± 0.08	1.5	1.2
pT/tA$_1$	T	0.90 ± 0.32	0.41 ± 0.06	0.46	0.59
pT/tA$_2$	T	0.82 ± 0.31	0.48 ± 0.20	0.58	0.45

[a] Reactions were performed at 20 °C as described in Methods using 5 nM Klenow exo⁻ (D335A, E357A) and 70 nM primer/template. Refer to Chart II for oligonucleotide sequences. [b] Values are listed for the slope of the linear region of [dAPTP] vs rate plots.

(Guest *et al.*, 1991b). The triphosphate group most likely quenches the AP fluorescence to some extent. When AP is present at the 3′-primer terminus in duplex DNA, there is a large decrease in the fluorescence lifetime (Figure 1b). Four lifetime components are required to fit the data, similar to previous reports for AP at the center of duplex DNA (Guest *et al.*, 1991b; Nordlund *et al.*, 1989). The fluorescence lifetime increases for AP at the 3′-primer terminus of duplex DNA when AP is bound to KF⁻ (D355A, E357A), which corresponds with the ≈2.5-fold enhancement of steady-state fluorescence for the KF⁻–DNA complex over free DNA (Figure 1a,b).

A single rotational correlation time (0.163 ns) was obtained from free dAPTP. When located at the 3′-primer terminus in DNA duplexes, AP exhibited long (~3–6 ns) and short (0.15–1 ns) rotational correlational times which compare well with a previous study (Guest *et al.*, 1991b) (Figure 1c). The shorter correlation times are most likely due to AP base motion, while the longer times can be ascribed to some component of the overall motion of the 17/30mer primer/templates. There is a dramatic increase in the long rotational correlation time for double-stranded DNA containing AP at the 3′-primer terminus when bound to KF⁻ (D355A, E357A). This long rotational correlation time (~42 ns) probably reflects the overall motion of the large (69 kD) KF⁻–DNA complex. A shorter rotational correlation time is also present for the complex, and it is similar in magnitude to the one found for double-stranded DNA alone and probably reflects AP base motion within the complex.

Steady-State and Pre-Steady-State Incorporation of dAPMP Measured by Fluorescence Spectroscopy. The kinetics of insertion of dAPMP by KF⁻ can be measured by following the decrease in the steady-state fluorescence emission of AP during the time course of a reaction. Data for reactions on each primer/template were normalized to the total change in AP fluorescence. The difference in insertion rates on the five templates can be seen clearly in Figure 2. Changing the downstream neighbor on the template from A (Figure 2, tA$_1$) to G (Figure 2, tA$_2$) does not affect the insertion efficiency significantly. Rates were calculated by linear fits to data from reaction time courses at early times. Kinetic constants were calculated from plots of the observed rate of insertion versus dAPTP concentration. A typical plot is shown in the inset to Figure 2, and kinetic constants for insertion of dAPMP are given in Table I. The relative rates of insertion of dAPMP, given by the ratios of [dAPTP]k_{cat}/K_m on different primer/templates, are slowest next to T. Changes in the relative insertion efficiencies of dAPMP next to different 5′-nearest neighbors result primarily from changes in k_{cat}. Values of apparent K_m range from 0.78 to 1.1 μM, while k_{cat} values range from 0.41 s^{-1} next to T to 2 s^{-1} next to G. Similar results were obtained by using higher [dAPTP] and DNA/enzyme ratios. Values of k_{cat} and K_m for insertion on pC/tG were 0.95 s^{-1} and 1.3 μM, respectively, in reactions containing 5 nM KF⁻ (D355A, E357A), 500 nM DNA, and 0.5–12 μM dAPTP.

Kinetics of insertion of dAPMP were measured for two primer/templates (pC/tG and pT/tA$_1$) under pre-steady-state conditions (see Experimental Procedures) where KF⁻ and primer/template were preincubated to form an enzyme–DNA complex before dAPTP was added (Figure 3). The relative efficiency of insertion given by the slope of the linear region of plots of rate versus [dAPTP] was greater next to nearest neighbor C (k_{cat}/K_m = 0.60 s^{-1}) than next to nearest neighbor T (k_{cat}/K_m = 0.27 s^{-1}). These rates are on the same order of magnitude as in steady-state experiments and show the same trend (i.e., insertion next to C is more efficient than insertion next to T).

The change in the steady-state fluorescence of 2-aminopurine during an enzyme-catalyzed reaction can be attributed to incorporation of free 2-aminopurine into a DNA primer/template and not to alternative modes of quenching, for the following reasons. (1) The decrease in AP fluorescence follows the stoichiometry of the reactions. For example, if a reaction mixture contained 1.2 μM dAPTP and 300 nM DNA, the observed decrease in the AP fluorescence was consistent with the incorporation of 1/4 of the dAPTP into DNA. (2) The

Table II: Kinetic Constants and Misinsertion Frequencies for Insertion of dAMP or dAPMP opposite a Template T by Klenow exo⁻ (D424A) Determined Using the Gel Assay with a DNA Trap[a]

primer/ template	5′-nearest neighbor	dNMP	K_m (μM)	$(I_2/I_1)_{max}$	k_{cat} (s^{-1})	k_{cat}/K_m ($\mu M^{-1}\ s^{-1}$)	f_{ins}
up/tC	G	A	0.97 ± 0.44	22 ± 3	5.6 ± 0.7	6.8 ± 2.4	1
		AP	2.7 ± 0.8	19 ± 2	5.0 ± 0.6	2.0 ± 0.4	0.31 ± 0.06
up/tG	C	A	0.93 ± 0.37	21 ± 6	3.8 ± 1.1	4.3 ± 0.5	1
		AP	4.6 ± 2.6	22 ± 9	4.0 ± 1.7	1.0 ± 0.2	0.23 ± 0.02
up/tA_1	T	A	0.48 ± 0.13	56 ± 11	2.1 ± 0.4	4.5 ± 0.4	1
		AP	2.7 ± 0.1	46 ± 5	1.7 ± 0.2	0.63 ± 0.05	0.15 ± 0.03
up/tA_2	T	A	0.34 ± 0	38 ± 5	0.83 ± 0.10	2.4 ± 0.3	1
		AP	2.5 ± 0.4	32 ± 5	0.69 ± 0.10	0.28 ± 0	0.12 ± 0.02

[a] Reactions were performed at 20 °C as described in Methods using 23 nM Klenow exo⁻ (D424A) and 50 nM running-start primer/templates. Results are the average of two separate experiments. Refer to Chart II for oligonucleotide sequences.

Table III: Kinetic Constants and Misinsertion Frequencies for Insertion of dAMP or dAPMP opposite a Template T by Klenow exo⁻ (D355A, E357A) Determined Using the Gel Assay with a DNA Trap[a]

primer/ template	5′-nearest neighbor	dNMP	K_m (μM)	$(I_2/I_1)_{max}$	k_{cat} (s^{-1})	k_{cat}/K_m ($\mu M^{-1}\ s^{-1}$)	f_{ins}
up/tC[b]	G	A	0.41 ± 0.06	19 ± 0	4.6 ± 0	11 ± 2	1
		AP	1.8 ± 0.1	16 ± 1	4.1 ± 0.2	2.3 ± 0.02	0.20 ± 0.02
		A vs AP[c]					0.23 ± 0.01
up/tG	C	A	0.31	14	1.6	5.0	1
		AP	1.9	16	1.8	0.92	0.18
up/tA_1	T	A	0.20	59	0.64	3.2	1
		AP	0.95	45	0.50	0.52	0.16

[a] Reactions were performed at 20 °C as described in Methods using 12 nM Klenow exo⁻ (D355A, E357A) and 50 nM running-start primer/templates. Refer to Chart II for oligonucleotide sequences. [b] Results are the average of two separate experiments. [c] Results from direct competition reaction under the same conditions as separate kinetic reactions, as described in Methods.

decrease in AP fluorescence follows the stoichiometry of the reaction regardless of whether the polymerase is present in stoichiometric amounts with the DNA or the DNA is in a large excess, indicating that there is no nonspecific binding of the AP to the polymerase causing the observed quenching. (3) In a reaction containing 100 nM dAPTP, 80 nM up/tC, and 5 nM KF⁻ where dAPMP was *not* incorporated opposite a C in template tC (data not shown), no decrease in AP fluorescence was observed, which further indicates that there is no nonspecific binding of AP to enzyme–DNA or bleaching of AP on the time scale of the reaction that leads to a decrease in AP fluorescence. (4) In reactions where dATP was allowed to compete with dAPTP for insertion (data not shown) both the observed rate of dAPMP incorporation and the total incorporation of dAPMP decreased as predicted from the gel competition assay (see Table III). (5) Time-resolved rotational anisotropies and total intensity decays measured on completed reactions containing an excess of DNA over enzyme are consistent with those observed for AP at the 3′-primer terminus of synthetic primer/templates.

The differences in the intensities of AP at the 3′-terminus of a synthetic duplex free in solution or bound to KF⁻ are small compared to the intensity of dAPTP. AP fluorescence increases by 2.5-fold when a synthetic primer/template containing AP at the 3′-primer terminus is bound to KF⁻ (Figure 1a), compared with a 25–125-fold decrease in fluorescence between free dAPTP and AP in duplex DNA. Thus, the observed quench in AP fluorescence does not arise as a result of release of the DNA product containing AP from the enzyme to an aqueous environment. We cannot rule out the possibility that the fluorescence of AP is quenched when it binds to the enzyme–DNA complex in a conformation where it is base paired with the template, stacked with the primer terminus, and poised for phosphodiester bond formation. It seems likely that the AP insertion rates may reflect a slower step than phosphodiester bond formation, e.g., a conformational change that orients the substrates in position to react (Kuchta *et al.*, 1987).

Biphasic reaction kinetics, which would indicate that the first turnover of enzyme–DNA substrate to enzyme–DNA product was faster than subsequent rounds of synthesis, were not observed for any of the DNA sequences. The rate constants for polymerization (k_{cat} values) are similar for both the steady-state and the pre-steady-state experiments, indicating that both types of experiment are measuring the same kinetic step. In a single-turnover experiment containing 1 μM KF⁻ (D355A, E357A) and 0.5 μM DNA (pT/tA_1), a value of k_{cat}/K_m = 0.63 s^{-1} was measured, which is similar to that obtained in the steady-state experiments (Table I). These results indicate that the observed rate is less than or equal to the rate of release of DNA product from polymerase.

Gel Assay Run under "Single Completed Hit" Conditions. Kinetics of insertion for both dAPMP and dAMP next to different base-stacking partners were measured using a gel assay (Boosalis *et al.*, 1987; Goodman *et al.*, 1993). When reactions are performed with a large excess of DNA primer/template in comparison with polymerase so that fewer than 20% of the labeled primers are extended, gel bands arise from a single encounter of a primer/template with a polymerase (single-hit conditions) (Goodman *et al.*, 1993). Under these single-hit conditions, fewer than 2% of primer/templates are extended more than once. Using the primer/template in large excess over the polymerase also ensures that observed band intensities contain an insignificant contribution from quenching of the reactions before the polymerase has completed synthesis on a given primer/template, thus stopping a polymerase prematurely (completed-hit conditions).

When polymerase reactions are performed under "single completed hit" conditions, the polymerase either inserts a nucleotide opposite the target site, measured by the intensity of the gel band at the target, or dissociates from the template prior to reaching the target, measured by the intensity of the

gel band at the template site prior to the target (Goodman *et al.*, 1993). The ratio of the band intensities (I_i/I_{i-1}) at the target site (site i) and the site immediately before the target site (site $i-1$) is a measure of the relative rates of extension of a primer from site $i-1$ to site i and dissociation at site $i-1$.[2] Another way to achieve single completed hit conditions is to run the reactions in the presence of a large excess of unlabeled trap DNA so that when the polymerase dissociates from the labeled DNA primer/template, it interacts with the large excess of unlabeled trap DNA rather than reassociating with labeled primer/template DNA. A plot of the observed ratio of band intensities, $(I_i/I_{i-1})_{obs}$, versus [dNTP] follows Michaelis–Menten kinetics and yields values for $(I_i/I_{i-1})_{max}$ and apparent K_m (Boosalis *et al.*, 1987):

$$(I_i/I_{i-1})_{obs} = \frac{(I_i/I_{i-1})_{max}[dNTP]}{[dNTP] + K_m} \quad (4)$$

The quantity $(I_i/I_{i-1})_{max}$ measures the ratio of the forward polymerization rate constant, k_{cat}, to the dissociation rate constant, k_{off} (at site $i-1$) (Goodman *et al.*, 1993). Thus, by measuring polymerase–DNA dissociation rates at site $i-1$, as described in the following section, we can calculate the slowest step, k_{cat}, along the pathway to extend a primer from site $i-1$ to i using eq 5.

$$k_{cat} = (I_i/I_{i-1})_{max}k_{off} \quad (5)$$

Mechanistic possibilities for this step include enzyme conformational changes (Kuchta *et al.*, 1987), translocation along the primer/template, and phosphodiester bond formation (Kuchta *et al.*, 1988). Product release rates cannot contribute to k_{cat} when reactions are carried out under single completed hit conditions.

Results for kinetics of insertion measured in the presence of a DNA trap are similar for both exonuclease-deficient mutants of Klenow (Table II for the single mutant, D424A, and Table III for the double mutant, D355A, E357A). Rate constants for dAMP insertion (k_{cat}), calculated by using eqs 4 and 5, are similar to those for insertion of dAPMP on the same primer/template for each polymerase. Values of K_m for insertion of dAPMP are about 4–8-fold larger than K_m values for insertion of dAMP, while k_{cat} values differ by only about 5–30%. Thus, misinsertion of dAPMP depends more on differences in K_m than on differences in k_{cat}. In agreement with the fluorescence data for insertion of dAPMP (Figure 2), rates of insertion of both dAPMP and dAMP are faster following a primer terminus G or C than a primer terminus T.

Polymerase Dissociation Rates from Primer/Templates. In order to calculate k_{cat} (eq 5) and make comparisons between k_{cat} values for insertion of dNTPs on primer/templates of different sequences, it is necessary to measure k_{off} since this rate constant changes with different DNA sequences. For these reactions, a solution of KF$^-$ was preincubated with a 5′-^{32}P-labeled primer annealed to unlabeled template before a solution of the unlabeled running-start dNTP and an excess of trap DNA were added. After a delay time between 0 and 150 s, a solution of a saturating concentration (51 μM) of dATP was added. During the delay time, some of the enzyme remained bound to the primer/template while some of the enzyme dissociated and interacted with the excess trap DNA. The polymerase that remained bound to primer/template was extended to the target T site in the presence of dATP. A gel showing the results of a typical k_{off} determination appears in Figure 4a. The fraction of polymerase remaining bound to the primer/template at any given delay time is equal to $I_i/(I_i + I_{i-1})$. A plot of $I_i/(I_i + I_{i-1})$ versus the delay time decays as a first-order exponential with rate constant k_{off} (Figure 4c) (Goodman *et al.*, 1993).

Dissociation rates were measured for both KF$^-$ mutants. The rate of dissociation (measured in two separate experiments for each primer/template) of KF$^-$ (D424A) is slightly faster when the primer ends in G (0.26 ± 0.02 s^{-1}) than when it ends in C (0.18 ± 0.01 s^{-1}), and about 7 times faster when the primer ends in G than in T (0.037 ± 0.006 s^{-1}), in reactions containing 5.6, 20, and 40 μM running-start dGTP, dCTP, and dTTP, respectively. Changing the base downstream of the target site from A (up/tA$_1$) to G (up/tA$_2$) reduces k_{off} by a factor of 1.7 to 0.022 ± 0.001 s^{-1}. Dissociation rates for the double mutant (D355A, E357A) show the same trend. Dissociation is faster following a primer terminus G (0.24 ± 0.02 s^{-1}) than following C (0.11 s^{-1}), and about 20 times faster following G than following T (0.011 s^{-1}), in reactions where running-start dNTP concentrations were 6.8, 6.9, and 6.7 μM for dGTP, dCTP, and dTTP, respectively. Large differences in dissociation rates also occur at different sites on the same primer/template. Dissociation of KF$^-$ (D424A) after insertion of dTMP (Figure 4a) on template tA$_1$ occurs at a rate of 0.037 ± 0.006 s^{-1}, while dissociation one base downstream after insertion of dAMP (Figure 4b,c) occurs at a rate we estimate to be at least 0.6 s^{-1}, or at least 16-fold faster.

Insertion Fidelity. Misinsertion efficiency (f_{ins}), given by the relative rates of insertion of incorrect (w) and correct (r) nucleotides, $f_{ins} = v(w)/v(r)$, can be deduced by measuring the kinetics of insertion of incorrect and correct nucleotides separately and then comparing the k_{cat}/K_m ratio for each (Fersht, 1985). When misinsertion kinetics are measured using the gel assay, the misinsertion efficiency is given by the relative insertion efficiencies of wrong and right in terms of $(I_i/I_{i-1})_{max}$,

$$f_{ins} = \frac{(k_{cat}/K_m)_w}{(k_{cat}/K_m)_r} = \frac{[(I_i/I_{i-1})_{max}/K_m]_w}{[(I_i/I_{i-1})_{max}/K_m]_r} \quad (6)$$

Note that it is not necessary to determine the enzyme dissociation rate, k_{off}, in order to calculate misinsertion efficiencies since the dissociation rate at site $i-1$ is the same regardless of the identity of the dNTP to be inserted at site i.

Misinsertion efficiencies next to different 5′-nearest neighbors for both KF$^-$ mutants were calculated by using eq 6 (Tables II and III). The greatest effect on f_{ins} of varying nearest neighbor primer termini in otherwise identical primer/template sequences was observed for the KF$^-$ (D424A) mutant polymerase, where AP insertion efficiencies were 0.31 ± 0.06, 0.23 ± 0.02, and 0.15 ± 0.03 next to G, C, and T, respectively. A change in the template base to the 5′-side of the target T site from A to G (Chart II) had little or no effect on the AP insertion efficiency next to primer T (Table II). Thus, as expected, the template cross-stacking perturbation appears to have less influence than the nearest neighbor interaction between the primer terminus and the incoming dNTP on the AP nucleotide insertion efficiency. There is a smaller difference in misinsertion efficiencies for KF$^-$ (D355A, E357A) on the different primer/templates. Misinsertion

[2] In cases where there is extension beyond the target site, the intensities of the bands extended to the target length and to greater than the target length must be summed ($(I_i + I_{i+1} + I_{i+2} + ...)/I_{i-1}$) to determine the relative rates of insertion at site i to polymerase dissociation at site $i-1$.

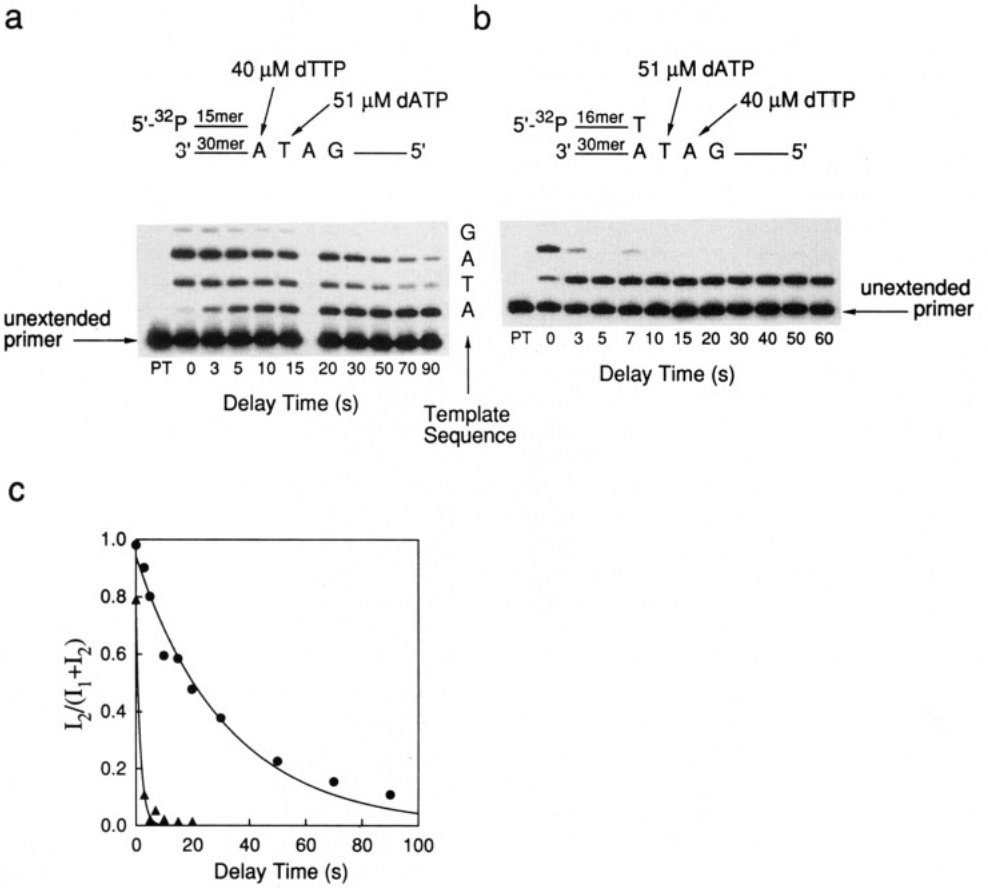

FIGURE 4: Measurements of k_{off} at two different sites on the same template, tA_1. (a) A gel showing measurement of KF⁻ (D424A) dissociation rate from up/tA_1 (15/30mer) after insertion of dTMP at 20 °C as described in Methods. Reaction mixtures contained 23 nM KF⁻ (D424A), 50 nM up/tA_1, 1 mg/mL trap DNA, 40 μM dTTP, and 51 μM dATP. (b) A gel showing dissociation of KF⁻ (D424A) following insertion of dAMP on pT/tA_1 (16/30mer). Reactions mixtures contained 23 nM KF⁻ (D424A), 50 nM pT/tA_1, 1 mg/mL trap DNA, 40 μM dTTP, and 51 μM dATP. (c) Plots of $I_2/(I_1 + I_2)$ versus time for the data in (a) and (b). For (a) the rate of dissociation following insertion of dTMP opposite A to form a 16mer is calculated where I_1 represents the intensity of the band due to the 16mer product and I_2 represents the sum of the band intensities for the 17mer and 18mer products. For (b) the dissociation rate following insertion of dAMP opposite T to form a 17mer is calculated where I_1 represents the intensity of the band due to the 17mer product and I_2 represents the intensity of the band due to the 18mer product. The plots decay as first-order exponentials from which k_{off} values of 0.031 s^{-1} for the 16/30mer (●) and >0.6 s^{-1} for the 17/30mer (▲) were calculated.

efficiencies next to nearest neighbor G, C, and T are 0.20 ± 0.02, 0.18, and 0.16, respectively.

Direct Competition Assay. We verified that the misinsertion efficiency deduced by measuring insertion kinetics for dAPMP and dAMP separately (eq 6) is equal to that obtained when dAPTP and dATP compete directly for insertion opposite T. Oligonucleotide products containing either 3′-terminus A or AP were clearly resolved by PAGE (Figure 5). The misinsertion frequency of 0.23 ± 0.01 found for direct competition was comparable to the misinsertion efficiency of 0.20 ± 0.02 determined by measuring kinetics separately.

Increase in Primer Utilization and Nucleotide Stimulation of Polymerase Dissociation. An unexpected observation was made concerning the extension kinetics of KF⁻ in the presence of dAPTP. When the gel assay was carried out in the absence of a trap under steady-state conditions using a large excess of DNA over polymerase and where each polymerase molecule must extend more than one primer/template, the rate of primer utilization increased as the concentration of dAPTP increased even though the concentration of the running-start base remained constant. This effect was especially pronounced for reactions with primers terminating in T (up/tA_1 and up/tA_2) and occurred to a smaller extent on the primer terminating in G (up/tC), but it was not observed on the primer terminating in C (up/tG). For example, during a 2-min reaction using up/tA_1 with 0.073 μM dAPTP about 5% of the primers were

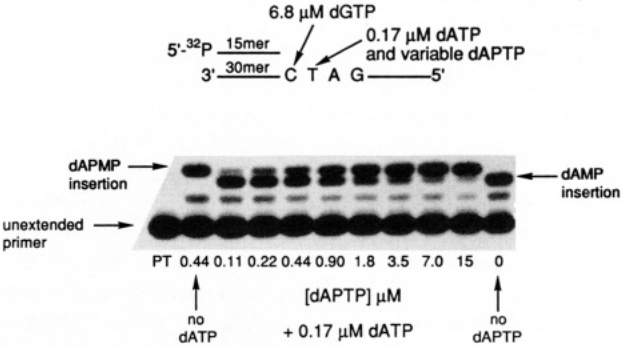

FIGURE 5: A gel showing the results of direct competition for insertion of dAMP and dAPMP into primer/template up/tC. Reaction mixtures contained a constant concentration (0.17 μM) of dATP and increasing concentrations of dAPTP as described in Methods. 5′-32P-Labeled 17mer products containing either a 3′-terminal A or AP were resolved by PAGE.

extended, but with 19 μM dAPTP about 30% of the primers were extended. The percentage of extended primers at intermediate concentrations increased as the concentration of dAPTP increased. These results imply that increasing the concentration of dAPTP, which is the second nucleotide to be inserted, increases the steady-state rate of primer utilization. It is not clear how the dAPTP is stimulating the rate of primer utilization by KF⁻ in an apparently sequence-dependent

manner. A similar observation was made for polymerase reactions with other mutants of Klenow fragment (Polesky *et al.*, 1992) and was attributed to dNTP-assisted polymerase–DNA dissociation.

Although product dissociation is not the rate-determining step in the extension of a single primer from site i – 1 to site *i*, it may be the rate-determining step in the overall steady-state cycle where a polymerase binds a primer/template, extends the primer, dissociates from that primer/template either before or after extension to site *i*, and then binds a *new* primer/template to continue the cycle. Dissociation rates for KF⁻ (D355A, E357A) bound to up/tA$_1$ were measured in the presence and absence of a ribonucleotide (GTP), which was not incorporated, to determine if high nucleotide concentrations could stimulate dissociation. Dissociation rates increased as the concentration of GTP increased. Values of k_{off} were 0.023, 0.039, and 0.065 s^{-1} for reactions which contained 0, 60, and 250 μM GTP, respectively. An increase in nucleoside triphosphate concentrations can apparently increase polymerase–DNA dissociation rates for these mutant polymerases; however, these nucleotide concentrations, which result in a 3-fold increase in the dissociation rate, are relatively high in comparison with the nucleotide concentrations used in kinetic assays.

Dissociation rates at site *i* – 1 and site *i* were also measured. During kinetics reactions, as the concentration of the target nucleotide is increased, the fraction of polymerase that dissociates at the site before the target site (site *i* – 1) decreases. If dissociation after insertion of the running-start nucleotide is significantly slower than dissociation after insertion of the target nucleotide, and if dissociation is the rate limiting step for steady-state primer utilization, as shown previously for insertion of correct dNTPs (Kuchta *et al.*, 1987), then the observed recycling time for polymerase will decrease as the fraction of polymerases dissociating after insertion of the target nucleotide increases. Thus, the rate of primer utilization will increase as the concentration of target nucleotide increases. Dissociation was measured on template tA$_1$ after insertion of dTMP and after insertion of dAMP or dAPMP (see above and Figure 4) and on tC after insertion of dGMP and after insertion of dAMP or dAPMP (data not shown). In both cases, dissociation was slower following insertion of the running-start base than following insertion of dAMP or dAPMP, which was too fast to measure. We estimate that dissociation rates following insertion of dAPMP on primer/templates pG/tC and pT/tA$_1$ by KF⁻ (D424A) must be greater than or equal to 0.7 and 0.5 s^{-1} for pT/tA$_1$ and pG/tC, respectively (assuming that reactions have progressed through 4 half-lives by the first time points at 4 and 5 s, respectively).

Both dNTP-dependent polymerase–DNA dissociation rates and different dissociation rates at different primer/template sites may be contributing to the observed increase in primer utilization. We have not observed a nucleotide stimulation effect with other polymerases, such as Sequenase (T7 DNA polymerase), avian myeloblastosis reverse transcriptase, or a 3′→5′ exonuclease-deficient mutant of T4 DNA polymerase, in similar assays (L. B. Bloom and M. F. Goodman, unpublished results).

DISCUSSION

Local DNA Sequence Effects on Insertion Kinetics. A main goal of this paper was to examine specific sequence effects on DNA polymerase reactions. Changing the identity of the base pair immediately 5′ to the nucleotide to be inserted had a significant effect on both insertion kinetics and misinsertion efficiencies. Because misinsertion efficiencies for AP are much larger than for natural nucleotides, it is a more sensitive probe for measuring differences in insertion due to differences in local DNA sequences. For KF⁻(D424A), we observed that misinsertion of dAPMP opposite T decreased to 0.31 ± 0.06, 0.23 ± 0.02, and 0.15 ± 0.03 for primers terminating with G, C, and T, respectively (Table II). Changing a downstream template base from A to G had a negligible effect on dAPMP insertion next to primer T. For the double mutant KF⁻ (D355A, E357A), differences in misinsertion efficiencies with different nearest neighbors showed a smaller variation, although the trend was similar (Table III). Misinsertion next to G (0.20 ± 0.02) is greater than misinsertion next to T (0.16). Misinsertion efficiencies for dAPMP by both KF⁻ mutants ranged between 0.12 and 0.31, which is higher than the average value of 0.15 reported for T4 DNA polymerase at other sites (Bessman *et al.*, 1974; Clayton *et al.*, 1979; Pless & Bessman, 1983). These differences in relative rates of insertion given by the ratios of k_{cat}/K_m for a given dNMP next to different base-stacking partners seem to arise predominantly from differences in the k_{cat} values, which vary by a factor of 7–8. Values for K_m differ by a factor of 2–3 for a given dNMP on different primer/templates.

Base-stacking interactions between the incoming nucleotide and the 3′-primer terminus are likely to be contributing to the observed changes in insertion kinetics. Melting temperatures (T_m's) have been calculated for DNA doublets which contain either A·T or AP·T base pairs (Petruska & Goodman, 1985). The relative values of T_m reflect the relative stabilities of the doublets, which are due largely to base-stacking interactions between the two base pairs. Calculated T_m's are 69.7, 46.4, 39.8, and 28.5 °C when the 5′-base-stacking partners for AP are G, C, A, and T, respectively, and 86.4, 54.7, 54.5, and 36.7 °C when the 5′-base-stacking partners for A are G, C, A, and T, respectively (Petruska & Goodman, 1985), indicating that relative base-stacking energies vary with the 5′-base-stacking partner in the order G > C > A > T. Quantum-yield measurements made on synthetic primer/templates with identical sequences to the products of insertion by KF⁻ are correlated with the calculated T_m's. Quantum yields increased as the 5′-nearest neighbor base-stacking partner to AP was changed as follows: G < C < A ≈ T. An increase in quantum yield reflects a decrease in the interactions between AP and its neighboring bases on the primer/template which quench AP fluorescence. These experimental results support the calculated T_m's and relative stabilities of the doublets. The relative rates of both dAPMP and dAMP insertion in primer/templates with different 5′-nearest neighbor base-stacking partners correlate with the melting temperatures of the DNA doublets and the relative quantum yields. As seen in Tables II and III, the relative rates of insertion of both dAPMP and dAMP vary with the 5′-nearest neighbor in the order G > C > T.

Local DNA sequence has a large effect on KF⁻–DNA dissociation rates as well as insertion kinetics. Sequence-dependent differences in dissociation rates have also been observed for KF⁺ (Kuchta *et al.*, 1987) and HIV-1 reverse transcriptase (Yu & Goodman, 1992). About a 7-fold difference in k_{off} was seen for KF⁻ (D424A) for a primer terminating in G (0.26 ± 0.02 s^{-1}) compared with a primer terminating in T (0.037 ± 0.006 s^{-1}), and about a 20-fold difference was seen for KF⁻ (D355A, E357A) for primers terminating in G (0.24 ± 0.02 s^{-1}) and T (0.011 s^{-1}). Changing the base in the single-stranded region of the primer/template immediately following the target site from A to G decreases

k_{off} by about a factor of 2 for KF$^-$ (D424A). KF has been shown to bind over 5–8 base pairs of the duplex region of the primer/template (Allen *et al.*, 1989; Guest *et al.*, 1991a) in addition to bases in the single-stranded region of the template, so it was initially surprising that a change in 1 base pair could result in a 7–20-fold change in dissociation rate. Changes in some bases in the DNA strand are likely to have a more significant effect than changes at other sites. Changes in the region close to the site where the new nucleotide is to be inserted and where binding interactions with the polymerase are likely to be stronger would be expected to have a greater effect on the dissociation rate than changes in other more distant sites. When these differences in dissociation rates are viewed in terms of free energy differences for the two reactions, the energy differences are relatively small, only about 1 kcal/mol.

Interpretation of Kinetic Constants Derived from the Gel Assay. When the gel assay is done in the presence of a DNA trap, reactions are the result of a single encounter of a DNA polymerase with a primer/template. The kinetic constants correspond to rate-limiting steps in extension of primer/templates from site $i - 1$ to site i and not product release. It is possible that the rate-limiting steps differ for different nucleotides and at different primer/template sites so that k_{cat} and K_m measured for one nucleotide or at one site may represent different mechanistic steps than k_{cat} and K_m measured for another nucleotide or at a different site. Misinsertion frequencies, however, are robust. The ratio of k_{cat}/K_m [or $(I_i/I_{i-1})_{max}/K_m$] for insertion of an incorrect and a correct nucleotide at the same site is a measure of the relative efficiencies of insertion (Goodman *et al.*, 1993).

Misinsertion efficiencies can be measured by direct competition of an incorrect nucleotide in the presence of a correct nucleotide, or they can be calculated, as in eq 6, from the values of k_{cat}/K_m [or $(I_i/I_{i-1})_{max}/K_m$] measured for each nucleotide separately (Boosalis *et al.*, 1987; Fersht, 1985). Misinsertion efficiencies for natural nucleotides are often hard to measure in direct competition experiments because they tend to be on the order of 10^{-3}–10^{-5}. Often concentrations of dNTPs are required which inhibit polymerase since the correct nucleotide must be maintained at a concentration in excess of the DNA concentration and a large pool bias of the incorrect nucleotide is required for the incorrect nucleotide to compete effectively for insertion. We have demonstrated that misinsertion efficiencies deduced by measuring kinetics for insertion of dAMP and dAPMP separately using the gel assay agree within experimental error with misinsertion efficiencies measured in direct competition. The misinsertion efficiency on primer/template up/tC was 0.23 ± 0.01 for dAPMP measured in direct competition with dAMP and 0.20 ± 0.02 from separate kinetics measurements (Table III).

2-Aminopurine as a Fluorescent Probe. Two methods for measuring polymerase kinetics were used in this study, fluorescence spectroscopy combined with rapid-mixing stopped-flow techniques and a gel fidelity assay. We found that rates and kinetic constants determined using pre-steady-state kinetic measurements were similar to those obtained from steady-state measurements.

AP has a much higher fluorescence intensity when present as a nucleotide than when present in DNA. We have shown that a decrease in AP fluorescence can be used to follow the kinetics of nucleotide insertion by a DNA polymerase, while a corresponding increase in fluorescence can be used to follow exonucleolytic removal of AP from a 3′-primer terminus (L. B. Bloom, M. R. Otto, Goodman, and Beechem, unpublished results). Although not extensively investigated in this study, the fluorescence of AP is also sensitive to interactions with KF$^-$. There is a small increase in fluorescence when double-stranded DNA containing AP at the 3′-primer terminus is bound to KF$^-$ and a corresponding increase in the rotational correlation time for AP in the complex.

Fluorescence spectroscopy is a powerful tool for studying DNA polymerase catalyzed reactions because dynamic information can be obtained about these reactions in real time. In combination with a fluorescent nucleotide analog such as 2-aminopurine, fluorescence spectroscopy can be used to follow polymerase-catalyzed reactions on a millisecond time scale, corresponding to single-turnover events for nucleotide insertion and removal. Another advantage of using AP as a fluorescent probe is that it does not appear to perturb DNA structure when paired opposite T (Nordlund *et al.*, 1989; Sowers *et al.*, 1986), unlike nucleotide analogs containing bulky fluorescent moieties. 2-Aminopurine's steric properties would be expected to be similar to normal nucleotides in the polymerase active site. Because the fluorescence properties of AP are sensitive to its environment and because it forms a reasonably good base pair with T, it may be a useful probe for studying dynamic interactions within DNA (Guest *et al.*, 1991b; Nordlund *et al.*, 1989) and dynamic interactions between other DNA binding proteins and AP-containing DNA.

Comparison of Fluorescence Measurements and the Gel Assay. A direct comparison of dAPMP incorporation kinetics was made using the fluorescence assay on both steady-state and pre-steady-state time scales and using the gel assay (Tables I–III). Results from all three assays were similar for the primer/templates used to measure the kinetics of insertion of dAPMP. Values for k_{cat}/K_m which correspond to the efficiency of insertion of 2-aminopurine ranged from 0.46 to 2.0 μM^{-1} s^{-1} (Table I) for the fluorescence assay under steady-state conditions and from 0.52 to 2.3 μM^{-1} s^{-1} for the gel assay (Table III). Values for k_{cat}/K_m measured under pre-steady-state conditions on primer/templates pC/tG and pT/tA$_1$ were 0.60 and 0.27 μM^{-1} s^{-1}, respectively, for KF$^-$ (D355A, E357A). Values of k_{cat} ranged from 0.41 to 2.0 s^{-1} for the fluorescence assay under steady-state conditions (Table I) and from 0.50 to 4.1 s^{-1} for the gel assay (Table III).

For the fluorescence assay, reactions were performed by preincubating the primer/template and enzyme and then initiating the reaction by the addition of dAPTP. If the first turnover of substrates to products occurred at a faster rate than subsequent turnovers, biphasic kinetics would have been observed in steady-state experiments where the ratio of enzyme to DNA was 1:14. Biphasic kinetics would indicate that a slower kinetic step occurred after incorporation of dAPMP that limited the steady-state rate of incorporation. We have measured the rate of insertion of dAPMP and the rate of dissociation following insertion of dAPMP. Insertion rates are relatively slow for dAPMP ($0.4 < k_{cat} < 5.0$ s^{-1} depending on sequence; Tables I–III), and dissociation rates are relatively high after insertion of dAPMP (estimated $k_{off} \geq 0.5$ s^{-1}), in comparison with rates of insertion and dissociation reported for the correct nucleotide (Kuchta *et al.*, 1987). The slow rate of insertion of dAPMP and the fast rate of dissociation are consistent with the apparent lack of biphasic kinetics and suggest that dissociation occurs at a rate similar to or faster than insertion, in contrast to the ≈800-fold greater rate of insertion than dissociation for the correct nucleotide (Kuchta *et al.*, 1987). If a small burst was obscured by noise in the data in experiments where a polymerase-to-DNA ratio of 1:14 was used, then we would have measured faster rates of insertion

in pre-steady-state experiments where enzyme-to-DNA ratios were higher (2:5 and 2:1). The similarity of the reaction rates measured in both pre-steady-state and steady-state experiments and the apparent lack of biphasic reaction kinetics suggest that both assays are measuring the same kinetic steps. Because the gel assay, done in the presence of a DNA trap, is the result of a single encounter of polymerase and DNA, all three assays are likely to be measuring steps in the reaction pathway that occur *prior* to release of product DNA (Goodman *et al.*, 1993). Mechanistic possibilities for this step include but are not limited to a conformational change in the enzyme, translocation along the DNA primer/template, and phosphodiester bond formation.

CONCLUSIONS

We have used two independent methods to measure insertion kinetics and fidelity for KF^- as a function of the 5′-nearest neighbor base-stacking partner. Previous kinetic studies have not examined in a systematic manner the sequence dependence of DNA polymerase nucleotide insertion rates. While the effects of 5′-nearest neighbor base composition were examined in only a single sequence context, it is clear that these small changes cause significant variations in insertion kinetics, fidelities, and dissociation rates for KF^-. It remains to be seen whether these results hold within other sequence contexts and using other polymerases. The fidelity of insertion by different polymerases may be affected differently and to varying degrees by nearest neighbor base-stacking partners and different local sequence contexts. Incorporation efficiencies of dAPMP by bacteriophage T4 antimutator L141 DNA polymerase have been shown to vary greatly at different sites, while those for wild-type T4 DNA polymerase and KF^+ vary to a smaller extent at those same sites (Pless & Bessman, 1983). Polymerases with different biological roles and from different organisms may use different mechanisms and kinetic steps to achieve fidelity of nucleotide insertion (Capson *et al.*, 1992; Kati *et al.*, 1992; Kuchta *et al.*, 1987, 1988; Patel *et al.*, 1991; Wong *et al.*, 1991). Relatively small differences in base-stacking energies can lead to relatively large differences in k_{cat}/K_m at different sites since $\Delta\Delta G = -RT \ln[(k_{cat}/K_m)_{site\ A}/(k_{cat}/K_m)_{site\ B}]$. It will be important to determine how local DNA sequence generally affects insertion kinetics and fidelity for DNA polymerases from different sources.

A novel method for studying polymerase-catalyzed reactions in real time which is based on fluorescence changes for 2-aminopurine in different environments has been introduced. The validity of this spectroscopic methodology has been shown by the similarity of results obtained by using a kinetic gel assay. The real-time spectroscopic approach, however, can provide additional information concerning intermediate states not observable by examination of product formation alone. Although not presented in this study, dynamic interactions between a polymerase and a 2-aminopurine substrate (either nucleotide or DNA containing AP) in the active site can be examined during the reaction. In this paper, we have shown that fluorescence quench of 2-aminopurine on a millisecond time scale can be used to measure nucleotide insertion kinetics, and depolarization of 2-aminopurine can be detected on a nanosecond time scale, corresponding to rotational diffusion, in the active cleft of Klenow fragment. This methodology can be applied to studies of a wide range of enzymes, such as other DNA and RNA polymerases, exonucleases (the increase in AP fluorescence can be followed as AP is excised), and polymerase accessory proteins, to measure reaction kinetics on a millisecond time scale and dynamic interactions between the enzymes and the AP substrates.

REFERENCES

Allen, D. J., Darke, P. L., & Benkovic, S. J. (1989) *Biochemistry 28*, 4601–4607.

Bessman, M. J., Muzyczka, N., Goodman, M. F., & Schnaar, R. L. (1974) *J. Mol. Biol. 88*, 409–421.

Boosalis, M. S., Petruska, J., & Goodman, M. F. (1987) *J. Biol. Chem. 262*, 14689–14696.

Capson, T. L., Peliska, J. A., Kaboord, B. F., Frey, M. W., Lively, C., Dahlberg, M., & Benkovic, S. J. (1992) *Biochemistry 31*, 10984–10994.

Clayton, L. K., Goodman, M. F., Branscomb, E. W., & Galas, D. J. (1979) *J. Biol. Chem. 254*, 1902–1912.

Derbyshire, V., Freemont, P. S., Sanderson, M. R., Beese, L., Friedman, J. M., Joyce, C. M., & Steitz, T. A. (1988) *Science 240*, 199–201.

Derbyshire, V., Grindley, N. D. F., & Joyce, C. M. (1991) *EMBO J. 10*, 17–24.

Echols, H., & Goodman, M. F. (1991) *Annu. Rev. Biochem. 60*, 477–511.

Eritja, R. E., Kaplan, B. E., Mhaskar, D., Sowers, L. C., Petruska, J., & Goodman, M. F. (1986) *Nucleic Acids Res. 14*, 5869–5884.

Fersht, A. R. (1985) in *Enzyme Structure and Mechanism*, W. H. Freeman and Co., New York.

Goodman, M. F., Creighton, S., Bloom, L. B., & Petruska, J. (1993) *Crit. Rev. Biochem. Mol. Biol. 28*, 83–126.

Guest, C. R., Hochstrasser, R. A., Dupuy, C. G., Allen, D. J., Benkovic, S. J., & Millar, D. P. (1991a) *Biochemistry 30*, 8759–8770.

Guest, C. R., Hochstrasser, R. A., Sowers, L. C., & Millar, D. P. (1991b) *Biochemistry 30*, 3271–3279.

Joyce, C. M. (1989) *J. Biol. Chem. 264*, 10858–10866.

Joyce, C. M., Chen Sun, X., & Grindley, N. G. (1992) *J. Biol. Chem. 267*, 24485–24500.

Joyce, C. M., & Grindley, N. D. F. (1983) *Proc. Natl. Acad. Sci. U.S.A. 80*, 1830–1834.

Kati, W. M., Johnson, K. A., Jerva, L. F., & Anderson, K. S. (1992) *J. Biol. Chem. 267*, 25988–25997.

Kuchta, R. D., Benkovic, P., & Benkovic, S. J. (1988) *Biochemistry 27*, 6716–6725.

Kuchta, R. D., Mizrahi, V., Benkovic, P. A., Johnson, K. A., & Benkovic, S. J. (1987) *Biochemistry 26*, 8410–8417.

Mendelman, L. V., Boosalis, M. S., Petruska, J., & Goodman, M. F. (1989) *J. Biol. Chem. 264*, 14415–14423.

Nordlund, T. M., Andersson, S., Nilsson, L., Rigler, R., Gråslund, A., & McLaughlin, L. W. (1989) *Biochemistry 28*, 9095–9103.

Patel, S. S., Wong, I., & Johnson, K. A. (1991) *Biochemistry 30*, 511–525.

Petruska, J., & Goodman, M. F. (1985) *J. Biol. Chem. 260*, 7533–7539.

Pless, R. C., & Bessman, M. J. (1983) *Biochemistry 22*, 4905–4915.

Polesky, A. H., Dahlberg, M. E., Benkovic, S. J., Grindley, N. D. F., & Joyce, C. M. (1992) *J. Biol. Chem. 267*, 8417–8428.

Setlow, P., Brutlag, D., & Kornberg, A. (1972) *J. Biol. Chem. 247*, 224–231.

Sowers, L. C., Fazakerley, G. V., Eritja, R., Kaplan, B. E., & Goodman, M. F. (1986) *Proc. Natl. Acad. Sci. U.S.A. 83*, 5434–5438.

Ward, D. C., Reich, E., & Stryer, L. (1969) *J. Biol. Chem. 244*, 1228–1237.

Wong, I., Patel, S. S., & Johnson, K. A. (1991) *Biochemistry 30*, 526–537.

Yu, H., & Goodman, M. F. (1992) *J. Biol. Chem. 267*, 10888–10896.